■ KNEE

Mapping the contact area of the patellofemoral joint

THE RELATIONSHIP BETWEEN STABILITY AND JOINT CONGRUENCE

D. Clark,
J. M. Stevens,
D. Tortonese,
M. R. Whitehouse,
D. Simpson,
J. Eldridge

From Avon Orthopaedic Centre, Bristol, United Kingdom

■ D. Clark, MBBS, FRCS, MSc, MD, Orthopaedic Surgeon
■ J. Eldridge, MBChB, BSc, FRCS, FRCS(T&O), Orthopaedic Surgeon
Avon Orthopaedic Centre, Southmead Hospital, Bristol, UK.

■ J. M. Stevens, MBBS, ChM, PGDip, FRACS, FAOrthA, Orthopaedic Surgeon, Knox Orthopaedic Group, Knox Private Hospital Melbourne, Melbourne, Australia.

■ D. Tortonese, DVM, PhD, Senior Lecturer in Anatomy, Centre for Applied Anatomy, University of Bristol, Bristol, UK.

■ M. R. Whitehouse, PhD, MSc, BSc, MBChB, FRCS(T&O), PG Cert(HE), FHEA, Orthopaedic Surgeon, Avon Orthopaedic Centre, Southmead Hospital, Bristol, UK; Musculoskeletal Research Unit, Translational Health Sciences, Bristol Medical School, Southmead Hospital, Bristol, UK; National Institute for Health Research, Bristol Biomedical Research Centre, University Hospitals Bristol NHS Foundation Trust and University of Bristol, Bristol, UK.

■ D. Simpson, BSc, Medical Student, University of Nottingham Medical School, Queen's Medical Centre, Nottingham, UK.

Correspondence should be sent to J. M. Stevens; email: drjarradstevens@hotmail.com

doi:10.1302/0301-620X.101B5.BJJ-2018-1246.R1 $2.00

Bone Joint J 2019;101-B:552–558.

Aims

The aim of this study was to determine and compare the congruency of the articular surface contact area of the patellofemoral joint (PFJ) during both active and passive movement of the knee with the use of an MRI mapping technique in both the stable and unstable PFJ.

Patients and Methods

A prospective case-control MRI imaging study of patients with a history of PFJ instability and a control group of volunteers without knee symptoms was performed. The PFJs were imaged with the use of an MRI scan during both passive and active movement from 0° through to 40° of flexion. The congruency through measurement of the contact surface area was mapped in 5-mm intervals on axial slices. In all, 40 patients were studied. The case group included 31 patients with symptomatic patellofemoral instability and the control group of nine asymptomatic volunteers. The ages were well matched between the case and control groups. The mean age was 25 years (16 to 42; SD 6.9) in the case group and 26 years (19 to 32; SD 5.1) in the control group. There were 19 female and 12 male patients in the case group.

Results

The unstable PFJs were demonstrably less congruent than the stable PFJs throughout the range of knee movement. The greatest mean differences in congruency between unstable and stable PFJ's were observed between 11° and 20° flexion (1.73 cm^2 *vs* 4.00 cm^2; $p < 0.005$).

Conclusion

The unstable PFJ is less congruent than the stable PFJ throughout the range of knee movement studied. This approach to mapping PFJ congruency produces a measurable outcome and will allow the assessment of pre- and postoperative results following surgical intervention. This may facilitate the design of new procedures for patients with PFJ instability. If a single axial series is to be obtained on MRI scan, the authors recommend 11° to 20° of tibiofemoral flexion, as this was shown to have the greatest difference in contact surface area between the case and control groups.

Cite this article: *Bone Joint J* 2019;101-B:552–558.

The patellofemoral joint (PFJ) is geometrically complex, asymmetric, and heavily influenced by kinematic forces about the knee. Patella engagement and subsequent congruence of the patella within the trochlear groove provides stability and the dispersion of force across the articulating surfaces throughout the arc of movement.

In 1976, Goodfellow et al[1] described changes to the contact area that occur in the normal knee with movement, with the distal patella engaging in extension while the proximal patella articulating in flexion. In the unstable PFJ, the patella will move in an abnormal manner, potentially producing an uneven distribution of forces. This may present clinically as subluxation and/or dislocation of the patella. Incongruency of the PFJ, even without patella instability, may lead to degenerative changes.[2-7]

Visualizing the congruency of the PFJ with imaging studies is useful for diagnosis, planning operative intervention, and evaluating postoperative outcomes.[8] Methods for assessing the PFJ include plain radiographs, ultrasound scanning,

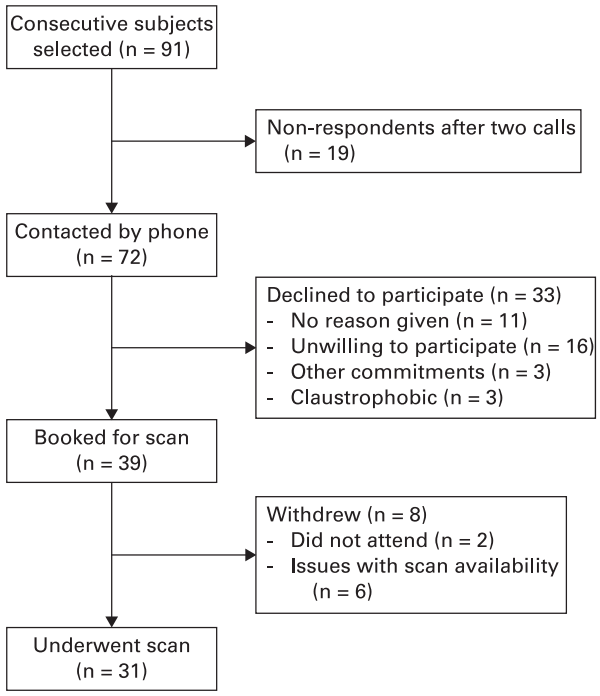

Fig. 1

Flowchart of case/patient inclusion and exclusion.

CT, MRI, and 3D computer navigation.[8-12] Accurate assessment of the congruency of the PFJ is key in understanding the relationship of the bone and cartilage architecture, force vectors about the joint, and the soft-tissue restraints.

In order to improve objective MRI analysis of the unstable PFJ, we sought to map the contact area through a range of passive and active movement. Although this technique is not designed to be a routine investigation, we have undertaken this study to produce direct quantifiable measurements in patients with an unstable PFJ. We also performed this analysis in a control group of stable knees for comparison, in order to document the normal contact area throughout the range of movement under study. Our hypothesis was that the unstable PFJ will be less congruent than the stable joint through both a passive and an active range of movement with quadriceps contraction, when mapped on multiple sequence MRI scans.

The aims of the study were: 1) to describe the articulating surface area of the PFJ in both active and passive movement; and 2) to compare joint contact area using this method for stable and unstable PFJs.

Patients and Methods

This study was given ethical approval from NRES Committee South West – Frenchay, United Kingdom (12/SW/0155) and all participants gave written informed consent. A single-centre, prospective case-control MRI imaging study of patients with PFJ instability (case group, n = 31) and volunteers with no PFJ symptoms (control group, n = 9) was performed. An MRI scan was used to capture and measure the PFJ articular cartilage contact area at varying degrees of knee flexion both in passive movement and with active quadriceps contraction for both groups.

The group size was calculated by a two-sample independent-samples Student's *t*-test with a mean difference of 2 cm^2 (SD 1.75), power of 80%, type I error = 0.05, and a sampling ratio of 3:1 (case:control groups) yielding a minimum required sample size of 27 patients in the case group and nine patients in the control group. We recruited 31 patients in the case group and nine patients in the control group.

Inclusion criteria for the case group included patients with PFJ instability who were waiting for surgical treatment. The diagnosis of instability was based on history (which included at least two prior episodes of patella dislocation), examination, and imaging investigations. The control group was recruited from healthy volunteers, who reported no PFJ symptoms currently or previously and demonstrated normal knee examination with no clinical signs of instability.

The exclusion criteria included patients who were unable to provide valid consent, were unwilling to participate, were aged 17 years or less, suffered from degenerative knee joint disease (including any evidence of osteoarthritis on radiographs in antero-posterior, lateral and skyline views), were pregnant, had a history of metal objects or the possibility of metal object in soft tissues (e.g. brain, eye, heart, or spinal cord), or if they were not contactable by telephone.

The case subjects were recruited from the patient waiting list for surgery at a tertiary elective orthopaedic unit. In all, 91 consecutive patients were considered to be potentially eligible case subjects based on inclusion criteria. Of these, 72 were willing to discuss the study and 39 agreed to participate. There were eight patient withdrawals, leaving a group size of 31 (Fig. 1).

The ages were well matched between the case and control groups. The mean age was 25 years (16 to 42; SD 6.9) in the case group and 26 years (19 to 32; SD 5.1) in the control group (p = 0.690; Table I). There were 19 female and 12 male patients in the case group (p = 0.060; Table II).

Information regarding age, symptoms, previous dislocations, hypermobility, and imaging results (Tibial Tuberosity Trochlear Groove, Insall–Salvati Ratio, Biedert Patellotrochlear Index, Dejour grade) were obtained from patient notes and the Picture Archiving and Communications Systems (PACS).

The control group was used to define normal values and validate the study methodology. Nine healthy volunteers were recruited from the hospital staff and our knee research group who demonstrated normal knees and no history of PFJ symptoms. No formal imaging prior to the study MRI scans was organized for the volunteers in the control group.

MRI scanning protocol. MRI was performed with a GE Discovery MR450 1.5 Tesla scanner (GE Healthcare, Waukesha, Wisconsin) and an eight-channel cardiac coil. The subject underwent a standard checklist, for which they were asked specific questions regarding comfort and safety in the MRI scanner.

Patient position. The subject lay supine on the MRI table with a triangular wedge under the knee and a strap over the thighs in order to maintain the position of the femur during the examination (Fig. 2a). Data was captured in both passive and in active movement with quadriceps contraction.

The initial localizer MRI sequence performed was an ultrafast gradient echo 3 plane localizer. The localizer scan permitted the technician to identify the boundaries of the trochlea and

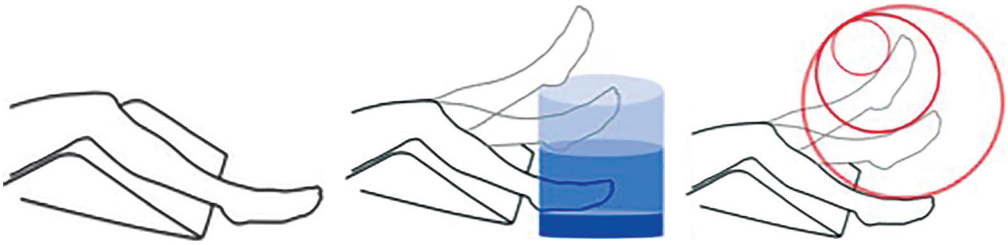

Fig. 2a Fig. 2b Fig. 2c

a) The subject lay supine on the MRI table with a triangular wedge under the knee. b) Foam blocks were placed for passive range of movement at 0°, 20°, and 40° flexion. c) Deflating balloon against resistance with multiple sequence scans for active quadriceps contraction.

plan the location of the definitive scan. The scan boundaries were placed beyond the boundaries of the trochlea in order to ensure full capture of the area of interest. Blocks of axial images were captured with one sagittal localizer sequence to calculate the precise knee flexion position. The axial image was centred over the trochlea and then the patella was visualized as the knee extended, maintaining at all times the same series of images of the trochlea.

Passive movement imaging. The patient was secured as above, and the knee was permitted to rest at 40° of flexion; a series of images were then captured. A further foam cushion was placed under the heel to attain a scan at 20° of flexion. Finally, a further cushion was placed to attain a scan at 0° of flexion and the series was repeated (Fig. 2b). The angle of flexion was measured from the tibiofemoral angle on the sagittal localizer image as opposed to the thigh-calf angle used to position the patient.

Active quadriceps contraction imaging. The patient was positioned supine with a triangular foam pillow under the knee. A beach ball was placed anterior to the tibia with a valve under the control of the subject (Fig. 3). The subject was asked to extend the knee, pushing the lower leg against the balloon and causing it to deflate (Fig. 2c). Subjects were advised that it would be expected to take two minutes to achieve this. The MRI operator informed the subject that the scan was due to start so as to coincide this with the beginning of the scan. As the knee extended the scan was commenced and repeated while the subject deflated the balloon.

Rapid sequence axial images were captured while the ball was permitted to continue to deflate under the subject's control. The deflation rate was dependent upon the exertion of the patient and was not externally controlled. Five to eight sequences were captured per deflation.

Imaging sequence. After the localizer scan identified the distal femur, the sequence placement was planned so that the entire trochlea could be imaged. In both the active and passive modes, the thigh did not move due to control by strapping and it was possible to attain adequate quality imaging of the trochlea, without movement artefact. In each sequence, images captured included one sagittal slice and 10 to 18 axial slices (dependent on patient size) at 5 mm intervals.

In any given scan, up to five images demonstrated contact between the patella and the trochlea and at any given moment, the entire trochlea was captured in order to ensure all the relevant images along the path of the patella were captured.

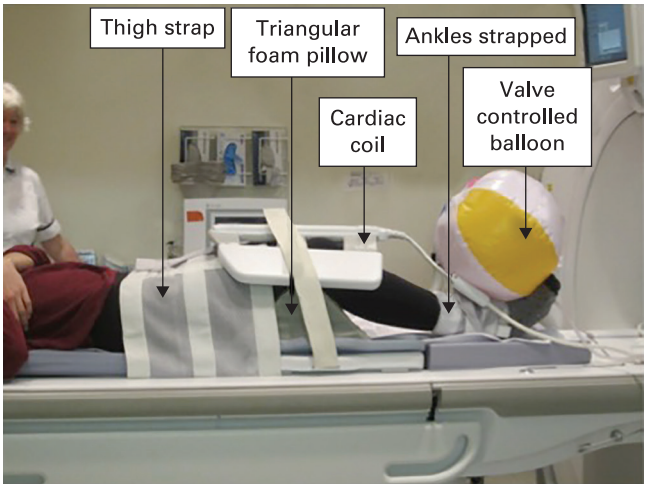

Fig. 3

A beach ball was placed anterior to the tibia to provide resistance and achieve quadriceps activation. The subject controlled a valve to control the rate of deflation.

Image interpretation. Using digital data supplied by the institutional PACS (GE Healthcare Centricity, Chicago, Illinois; Fujifilm Synapse, Tokyo, Japan), the operator manually identified boundaries of articular cartilage contact between the patella and femur on both sides of the trochlear sulcus on the axial view. These measurements were recorded as linear distances. Each slice is 5 mm wide and the surface area of each slice was calculated by multiplying the length by 5 mm. Each slice surface is then summed to reach a measure of the surface area in contact between the articulating surfaces to give a measure of congruency in each measurement condition. This was recorded on a 'flattened' 2D coronal plane image for visual interpretation of contact area (Fig. 4).

Statistical analysis. The repeatability of the measurements of MRI congruity were assessed by Pearson's correlation coefficient. The measurements were repeated by the primary investigator at a second timepoint, to give a measure of intraobserver error. The measurements were repeated by second observer for assessment of interobserver error. Comparison between case and control variables was made with a Fisher's exact test or chi-squared test for categorical variables depending upon number of groups or independent-samples Student's *t*-tests for

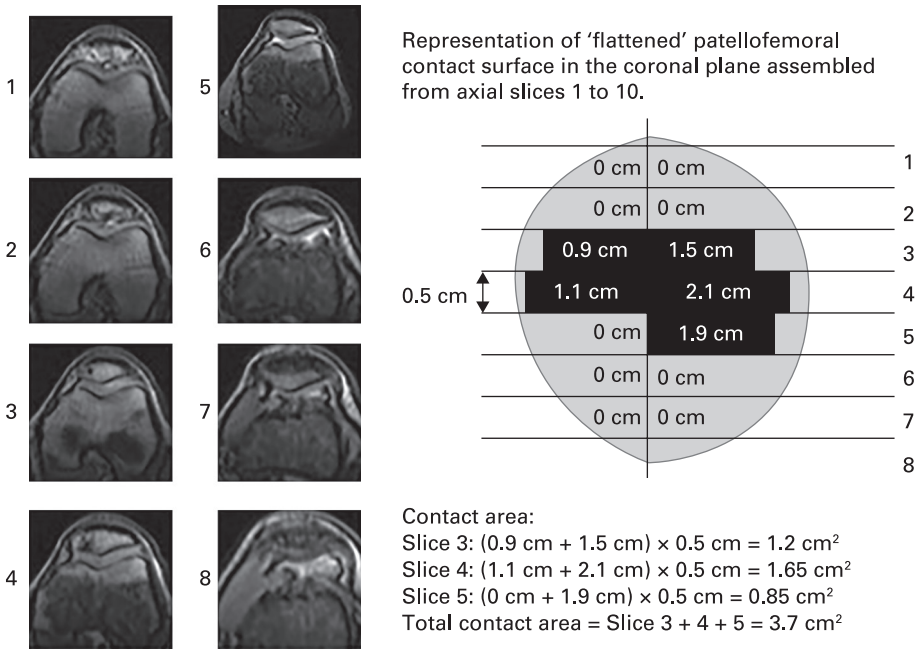

Fig. 4

'Flattening' of axial imaging. Slices are at 5 mm intervals. The width of each slice in which there is contact between the femur and patella cartilage is multiplied by 5 mm. Each measurement is then summed to give a total area of congruence.

Table I. Age, tibial tuberosity trochlear groove (TTTG) distance (mm), Insall–Salvati Ratio (ISR), and Biedert Patellotrochlear Index (BPI)

Variable	Case group	n	Control group	n	p-value*
Mean age, yrs (SD)	25 (6.9)	31	26 (5.1)	9	0.690
Mean TTTG (SD)	13.3 (4.6)	31	11.9 (3.2)	9	0.400
Mean ISR (SD)	1.37 (0.2)	31	1.19 (0.09)	9	0.013
Mean BPI (SD)	32.5 (23)	31	38.2 (3.3)	9	0.470
Mean age at first dislocation, yrs (SD)	14.9 (3.8)	21	N/A	N/A	N/A

*Independent-samples Student's *t*-test
N/A, not applicable

continuous data. Two-tailed independent-samples Student's *t*-tests were used to compare the mean joint congruence (cm^2) between the case and control groups during the different phases of knee flexion during quadriceps activation (0°, 0° to 10°, 11° to 20°, 21° to 30°, 31° to 40°, > 40°, and combined). All statistical analyses were performed using SPSS (IBM Corp., Armonk, New York).

Results

Laterality (side studied) was also well matched, with 36% being left among the patients in the case group and 44% among the patients in control group (p = 0.705). The other covariates of interest that are associated with the pathology were more frequent among the patients in the case group than those in the control group (Table III). All patients in the case group had sustained at least two dislocations, with 19 patients (61%) sustaining more than two dislocations. Seven patients (22.6%) in the case group had hypermobility with a Beighton score of four or more. Only six patients (19%) in the case group demonstrated a normal trochlear groove, with 14 patients (45%) displaying Dejour C abnormalities. Unsurprisingly, all control group patients demonstrated a normal trochlear groove.

The radiological measurements correlated strongly for intra-observer error (0.985) and for interobserver error (0.910). The line diagram illustrates that effect of quadriceps activation on congruence is limited to full extension amongst the normal population (Fig. 5). The histogram illustrates the trend from incongruence to congruency as the knee flexes (Fig. 6). The greatest differences in congruency between the case and control groups was seen in the active quadricep contraction group between the range of 0° and 20°. The greatest mean differences and greatest statistical significance was at the 11° to 20° range (p < 0.0001) (Fig. 6). The curves matched well between the case and control groups; the exception is at the 40+ range, where there only one case was recorded and the trend for increased congruence was not observed.

Discussion

The clinical relevance of this study was to establish a method for the direct measurement of PFJ contact area and congruency.

Table II. Clinical comparison between case and control groups

Variable	Case group, n (%)	Control group, n (%)	p-value*
Sex, female:male	19:12 (*61:39*)	2:7 (*22:78*)	0.060
Laterality, left:right	11:20 (*36:64*)	4:5 (*44:56*)	0.705
Dejour grade			
Normal	6 (*19*)	9 (*100*)	0.001
A	3 (*10*)	0 (*0*)	N/A
B	5 (*16*)	0 (*0*)	N/A
C	14 (*45*)	0 (*0*)	N/A
D	3 (*10*)	0 (*0*)	N/A
Hypermobile (Beighton Score of 4+)	7/31 (*22.6*)	0/9 (*0*)	0.175
Previous surgery	7/31 (*22.6*)	0/9 (*0*)	0.175
Subjects with > 2 dislocations	19/31 (*61*)	0/9 (*0*)	0.001

*Fisher's exact test or chi-squared test
N/A, not applicable

Table III. Comparison of mean joint congruence between the case and control groups during quadriceps active knee movement

Active quadriceps contraction: knee position, °	Case/control group	n	Mean joint congruence, cm^2 (SD)	Mean difference	95% CI	p-value*
< 0	Case	7	0.029 (0.76)	0.029	-0.10 to 0.16	0.626
	Control	2	0.00 (0)			
0 to 10	Case	26	0.59 (0.86)	-1.09	-1.80 to -0.38	0.004
	Control	11	1.68 (1.20)			
11 to 20	Case	26	1.73 (1.24)	-2.22	-3.16 to -1.27	< 0.001
	Control	9	4.00 (1.069)			
21 to 30	Case	24	3.13 (1.33)	-1.57	-2.64 to -0.49	0.006
	Control	8	4.70 (1.15)			
31 to 40	Case	18	3.85 (1.16)	-1.44	2.58 to -0.30	0.016
	Control	5	5.29 (0.65)			
40 +	Case	9	3.77 (1.51)	-0.83	-4.51 to 2.85	0.618
	Control	1	4.60 (N/A)			
Combined	Case	110	2.17 (1.76)	-1.24	-1.91 to -0.55	< 0.001
	Control	36	3.40 (1.90)			

*Independent-samples Student's *t*-test
CI, confidence interval; N/A, not applicable

With the ability to quantify congruency, the authors intend to use this technique to compare preoperative and postoperative contact areas in cases where stabilization surgery has been performed.

The results from this study will allow comparison of surgical cases to a baseline group of patients with stable knees. The range 11° to 20° (tibiofemoral angle) appears to be the most sensitive. Clinicians may use the routine MRI performed in this position to evaluate congruence by this technique.

The PFJ is a complex articulation for which accurate assessment of congruence and morphology may remain elusive using single imaging modalities or if viewed in a single plane.[13,14] Our sequential MRI scans demonstrated a close correlation between the measured contact area in the groups for both active and passive range of movement of the knee. When the case and control groups are compared, the mean contact area was greater in the control group through all ranges of movement, both in passive and with active quadriceps contraction, with the exception of quadriceps contraction in extension. This may be secondary to an abnormal articulation of the unstable patella within the trochlear by activation of the quadriceps muscles in this position.

The greatest mean differences between unstable and stable PFJ congruency during active quadriceps muscle contraction were observed between 11° and 20° (mean 1.73 cm^2 *vs* 4.00 cm^2; $p < 0.001$). This finding is important as lateral patellar displacement has been shown to occur, with the lowest displacing forces required, at 20° of knee flexion.[15]

Understanding articular contact area with different imaging modalities is problematic with significant mismatch between bony landmarks observed in radiographs or CT scans compared to the articular cartilage of the patella and trochlea landmarks seen on an MRI.[16] Patella position has been evaluated with the use of many different measures or indices such as the Insall–Salvati,[17] the modified Insall–Salvati,[18] the Blackburne–Peel,[19] the Caton–Deschamps,[20] and the Sagittal Patellofemoral Engagement Index.[21] Radiological classifications have been also reproduced with MRI.[22] While patellar height and engagement can be assessed in the sagittal plane, an appreciation of congruency especially through a range of movement is not possible.

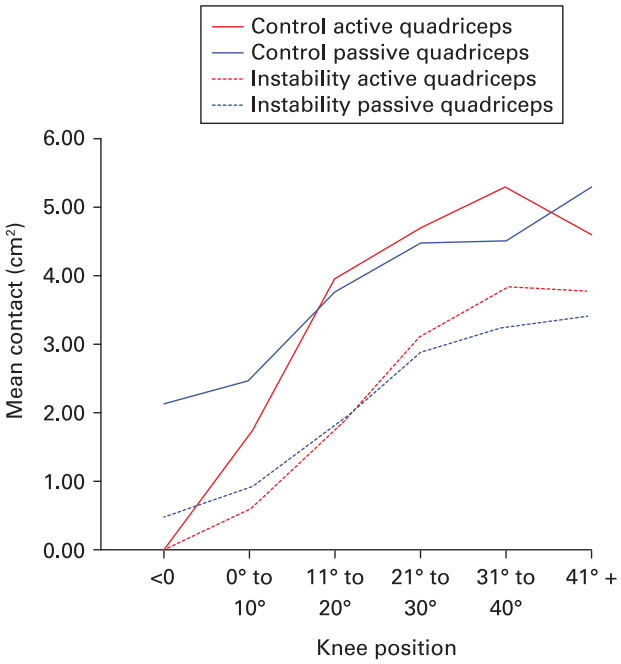

Fig. 5

Chart showing the control *versus* instability group in passive and active movement.

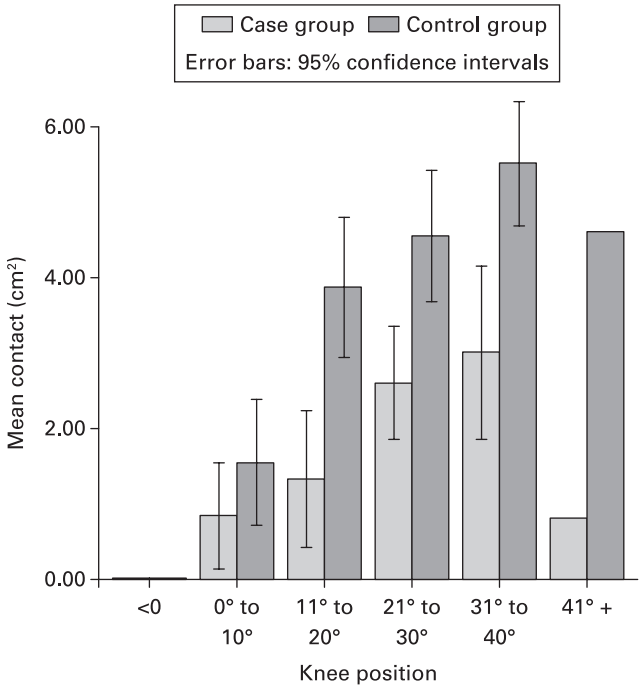

Fig. 6

Histogram showing quadriceps active movement, control, and instability.

Axial imaging provides information on the position of the patella within the trochlear groove; however, static knee position images provide little information toward the congruency or tracking through the range of movement. Skyline plain radiographs have been found to be unreliable,[23,24] as they can be difficult to obtain at degrees of knee flexion less than 30° where subluxation is most prevalent. It is for these reasons that we sought to evaluate the PFJ by means of measuring the contact area or congruence through axial MRI imaging during active movement, as cartilage contact is the functional basis of force transmission. Several other authors have previously given attention to activation of the quadriceps mechanism during capture of axial imaging.[24-26]

Brossmann et al[25] used dynamic MRI to analyze patella tracking in healthy volunteers and patients with maltracking. They reported significantly different patellar tracking patterns between the two groups and statistically significant tracking differences between static and dynamic scanning of the PFJ, although the contact surface area was not a measured outcome. While McNally et al[26] described the morphological traits of instability with dynamic axial MRI, there was no measurement of congruency or contact area. They demonstrated that patella subluxation was present in 40% of patients with anterior knee pain and challenged the clinical relevance of mild subluxation of the PFJ. Martinez et al[27] utilized CT scans at set intervals of 0°, 20°, and 45° of flexion to establish the effect of activation of the quadriceps on the centralization and tilt of the patella. The individuals assessed had asymptomatic knees and were considered healthy. They concluded that quadriceps contraction had little influence on the patellar centralization and did not affect patellar tilt unless in full extension. The effect of active quadriceps contraction on unstable PFJs was not explored by these authors.

We have sought to quantify the congruency of the PFJ through dynamic MRI mapping and using a 2D representation of the contact surface area. We have documented the difference in contact surface area between the stable and unstable PFJ. The potential of this MRI mapping method to establish and measure change in congruency for pre- and post-surgical intervention will allow for a more objective evaluation of treatment methods.

Our investigation has some limitations. Despite the small sample size in this study, there were significant differences in the contact area between 0° and 40° of knee flexion, when comparing the case and control groups. The imbalance of male patients (n = 7) to female patients (n = 2) in the control group is a weakness, as the majority of PFJ instability cases are seen in the female population. The addition of a dynamic element to MRI imaging has the potential for producing movement artefact, increasing the potential for difficulty in interpreting the data. Movement artefact was minimized by the use of rapid sequence MRI scanning, coupled with stabilization of the femur, and resulted in our study achieving clear and accurate images. Despite the risk of movement artefact, we believe dynamic imaging of the PFJ may be more representative of the conditions that are present during walking. The range of movement open to analysis was limited to 40° of flexion, due to the physical constraints of the MRI scanner.

The articulation of the PFJ, if accurately measured in terms of contact area, may provide useful information in determining the effectiveness of surgical treatment aimed at increasing joint congruency. We plan future studies, using this technique, to

compare patients pre- and post-surgical intervention, to quantify the effects of surgery on PFJ congruence.

In conclusion, the unstable PFJ is less congruent than the stable PFJ throughout knee movement. The unstable PFJ has reduced contact surface area and potentially increased contact pressure for a given force with an increased risk of degeneration of the joint. Mapping the contact area of the PFJ should allow a better understanding of joint congruence following surgical treatment and a measurement of the effectiveness of surgical intervention. If a single axial series is to be obtained on MRI scan, the authors recommend 10° to 20° of tibiofemoral flexion, as this was shown to have the greatest difference in contact surface area between the case and control groups.

Take home message

- The unstable patellofemoral joint (PFJ) is less congruent than the stable PFJ throughout range of knee movement.
- If a single axial series is to be obtained on MRI scan, the authors recommend 11° to 20° of tibiofemoral flexion.

References

1. **Goodfellow J, Hungerford DS, Zindel M.** Patello-femoral joint mechanics and pathology. 1. Functional anatomy of the patello-femoral joint. *J Bone Joint Surg [Br]* 1976;58-B:287–290.
2. **Dejour H, Walch G, Neyret P, Adelein P.** Dysplasia of the femoral trochlea. *Rev Chir Orthop Reparatrice Appar Mot* 1990;76:45–54. (Article in French)
3. **Eijkenboom JFA, Waarsing JH, Oei EHG, Bierma-Zeinstra SMA, van Middelkoop M.** Is patellofemoral pain a precursor to osteoarthritis? *Bone Joint Res* 2018;7:541–547.
4. **Luyckx T, Didden K, Vandenneucker H, et al.** Is there a biomechanical explanation for anterior knee pain in patients with patella alta? Influence of patellar height on patellofemoral contact force, contact area and contact pressure. *J Bone Joint Surg [Br]* 2009;91-B:344–350.
5. **Conchie H, Clark D, Metcalfe A, Eldridge J, Whitehouse M.** Adolescent knee pain and patellar dislocations are associated with patellofemoral osteoarthritis in adulthood: a case control study. *Knee* 2016;23:708–711.
6. **Utting MR, Davies G, Newman JH.** Is anterior knee pain a predisposing factor to patellofemoral osteoarthritis? *Knee* 2005;12:362–365.
7. **Clark D, Metcalfe A, Wogan C, Mandalia V, Eldridge J.** Adolescent patellar instability: current concepts review. *Bone Joint J* 2017;99-B:159–170.
8. **Keller JM, Levine WN.** Evaluation and imaging of the patellofemoral joint. *Oper Tech Orthop* 2007;17:204–210.
9. **Merchant AC, Mercer RL, Jacobsen RH, Cool CR.** Roentgenographic analysis of patellofemoral congruence. *J Bone Joint Surg [Am]* 1974;56-A:1391–1396.
10. **Øye CR, Holen KJ, Foss OA.** Mapping of the femoral trochlea in a newborn population: an ultrasonographic study. *Acta Radiol* 2015;56:234–243.
11. **Alemparte J, Ekdahl M, Burnier L, et al.** Patellofemoral evaluation with radiographs and computed tomography scans in 60 knees of asymptomatic subjects. *Arthroscopy* 2007;23:170–177.
12. **Wittstein JR, Bartlett EC, Easterbrook J, Byrd JC.** Magnetic resonance imaging evaluation of patellofemoral malalignment. *Arthroscopy* 2006;22:643–649.
11. **Victor J, Van Glabbeek F, Vander Sloten J, et al.** An experimental model for kinematic analysis of the knee. *J Bone Joint Surg [Am]* 2009;91-A(Suppl 6):150–163.
12. **Hashimoto S, Ochs RL, Komiya S, Lotz M.** Linkage of chondrocyte apoptosis and cartilage degradation in human osteoarthritis. *Arthritis Rheum* 1998;41;1632–1638.
13. **Saggin PR, Saggin JI, Dejour D.** Imaging in patellofemoral instability: an abnormality-based approach. *Sports Med Arthrosc Rev* 2012;20:145–151.
14. **Becker R, Hirschmann MT, Karlsson J.** The complexity of patellofemoral instability. *Knee Surg Sports Traumatol Arthrosc* 2018;26:675–676.
15. **Senavongse W, Farahmand F, Jones J, et al.** Quantitative measurement of patellofemoral joint stability: force-displacement behavior of the human patella in vitro. *J Orthop Res* 2003;21:780–786.
16. **Staeubli HU, Bosshard C, Porcellini P, Rauschning W.** Magnetic resonance imaging for articular cartilage: cartilage-bone mismatch. *Clin Sports Med* 2002;21:417–433.
17. **Insall J, Salvati E.** Patella position in the normal knee joint. *Radiology* 1971;101:101–104.
18. **Grelsamer RP, Meadows S.** The modified Insall-Salvati ratio for assessment of patellar height. *Clin Orthop Relat Res* 1992;282:170–176.
19. **Blackburne JS, Peel TE.** A new method of measuring patellar height. *J Bone Joint Surg [Br]* 1977;59-B:241–242.
20. **Caton J, Deschamps G, Chambat P, Lerat JL, Dejour H.** Patella infera. Apropos of 128 cases. *Rev Chir Orthop Reparatrice Appar Mot* 1982;68:317–325. (Article in French)
21. **Dejour D, Ferrua P, Ntagiopoulos PG, et al.** The introduction of a new MRI index to evaluate sagittal patellofemoral engagement. *Orthop Traumatol Surg Res* 2013;99(8 Suppl):S391-S398.
22. **Miller TT, Staron RB, Feldman F.** Patellar height on sagittal MR imaging of the knee. *Am J Roentgenol* 1996;167:339–341.
23. **Walker C, Cassar-Pullicino VN, Vaisha R, McCall IW.** The patello-femoral joint--a critical appraisal of its geometric assessment utilizing conventional axial radiography and computed arthro-tomography. *Br J Radiol* 1993;66:755–761.
24. **Inoue M, Shino K, Hirose H, Horibe S, Ono K.** Subluxation of the patella. Computed tomography analysis of patellofemoral congruence. *J Bone Joint Surg [Am]* 1988;70-A:1331–1337.
25. **Brossmann J, Muhle C, Schröder C, et al.** Patellar tracking patterns during active and passive knee extension: evaluation with motion-triggered cine MR imaging. *Radiology* 1993;187:205–212.
26. **McNally EG, Ostlere SJ, Pal C, et al.** Assessment of patellar maltracking using combined static and dynamic MRI. *Eur Radiol* 2000;10:1051–1055.
27. **Martinez S, Korobkin M, Fondren FB, Hedlund, LW, Goldner JL.** Computed tomography of the normal patellofemoral joint. *Invest Radiol* 1983;18:249–253.

Author contributions:
D. Clark: Conceptualized the study, Edited the data collection.
J. M. Stevens: Wrote the manuscript.
D. Tortonese: Conceptualized the study, Collected and edited the data.
M. R. Whitehouse: Analyzed and edited the statistics.
D. Simpson: Collected the data.
J. Eldridge: Conceptualized the study, Edited the manuscript, Supervised the study.

Funding statement:
Funding was provided by the David Telling Charitable Trust. This study was also supported by the NIHR Biomedical Research Centre at University Hospitals Bristol NHS Foundation Trust and the University of Bristol. The views expressed in this publication are those of the author(s) and not necessarily those of the NHS, the National Institute for Health Research, or the Department of Health and Social Care.

No benefits in any form have been received or will be received from a commercial party related directly or indirectly to the subject of this article.

Ethical review statement:
This study has ethical approval from NRES Committee South West – Frenchay, United Kingdom (12/SW/0155) and all participants gave written informed consent.

This article was primary edited by D. Johnstone.